

PREPRINT

Sensitivity Prewarping for Local Surrogate Modeling

Nathan Wycoff¹, Mickaël Binois² and Robert B. Gramacy¹

¹ Dept. of Statistics, Virginia Tech; ² ACUMES, Inria Sophia Antipolis

ARTICLE HISTORY

Compiled January 19, 2021

ABSTRACT

In the continual effort to improve product quality and decrease operations costs, computational modeling is increasingly being deployed to determine feasibility of product designs or configurations. Surrogate modeling of these computer experiments via local models, which induce sparsity by only considering short range interactions, can tackle huge analyses of complicated input-output relationships. However, narrowing focus to local scale means that global trends must be re-learned over and over again. In this article, we propose a framework for incorporating information from a global sensitivity analysis into the surrogate model as an input rotation and rescaling preprocessing step. We discuss the relationship between several sensitivity analysis methods based on kernel regression before describing how they give rise to a transformation of the input variables. Specifically, we perform an input warping such that the “warped simulator” is equally sensitive to all input directions, freeing local models to focus on local dynamics. Numerical experiments on observational data and benchmark test functions, including a high-dimensional computer simulator from the automotive industry, provide empirical validation.

KEYWORDS

computer experiments; emulation; sensitivity analysis; Gaussian process; dimension reduction; active subspace; subbagging

1. Introduction

As previously unimaginable computing power has become widely available, industrial scientists are increasingly making use of computationally intensive computer programs to simulate complex phenomena that cannot be explained by simple mathematical models and which would be prohibitively expensive to experiment upon physically. These computer experiments have varied business applications, for example: Zhou, et al. (93) describe virtualization of an injection molding process; Montgomery, et al. (60) explored the strength of automobile components via simulation; Crema, et al. (18) developed a computer model to help manage an assemble to order system.

To whom correspondence should be addressed: Nathan Wycoff (nathw95@vt.edu)

Despite the tremendous supply of computational resources provided by increasingly powerful CPUs, the general purpose GPU computing paradigm, and even more specialized hardware such as tensor processing units, the demands of advanced computer models are still sizeable. As such, there is a market for fitting surrogates to computer simulations: flexible statistical models which learn the input-output mapping defined by the simulator of interest, and are ideally suited to serve as a substitute for the same. For detailed review, see (30, 40, 75).

One popular use of computer experiments is to perform sensitivity analysis (e.g., 20, 38, 40, 59, 63, Ch. 8.2). This can consist of determining which of the input parameters are most influential, or even whether some latent combination of the inputs is driving the response. Sensitivity analysis for computer experiments must take into account unique characteristics not found in observational data. As in classical design of experiments, the training data inputs can be chosen, which means there is no need to take into account natural correlation between the input variables. Moreover, the design may be selected to maximize information gain or other criteria (40, Ch. 6). Further, in the case of deterministic experiments, we observe input-output dynamics exactly, and sometimes may even have derivative information (or can approximate it). Active Subspaces (AS; 15) exploit the knowledge of these gradients to perform linear sensitivity analysis, that is to say, sensitivity analysis which finds “directions”, or linear combinations of inputs, of greatest influence, rather than evaluating individual input variables. In this article, we will not assume knowledge of the gradient, but we will leverage that the target simulator is smooth, such that we can estimate its AS nonparametrically, as has been recently proposed (64–66, 91). These methods are closely related to existing gradient-based kernel dimension reduction (32) techniques from the statistics literature, which we discuss in a unified framework in Section 2.1.

Global Sensitivity Analysis (GSA), beyond being of interest in and of itself, can also be used to perform a transformation to the input space before applying standard modeling methods, a process referred to as premodeling in (53). Sometimes, this can take the form of variable selection, as in using lasso to select variables before fitting a standard linear model (3). Otherwise, the dimension of the space is not changed, but simply our orientation within it, for instance by changing basis to that implied by Principal Components Analysis (PCA). This has been recommended as a preprocessor for “axis-aligned” methods such as generalized additive models (23) and tree-based methods (73). And, of course, these approaches can be combined to learn both a rotated and truncated space, as in principal components regression (47).

In this article, we argue that this approach also has much promise as a preprocessor for local surrogate modeling of large-scale computer experiments (e.g., 41, 50). Practically speaking, what we dub “prewarping” influences the local model both directly and indirectly. Directly, because it redefines the definition of distances between points upon which many surrogate models (e.g., those based on Gaussian process regression) rely to compute relevant spatial correlations, and indirectly, as the definition of “lo-

cal” changes with the metric, thus influencing neighborhood selection. We build on recently proposed linear GSA techniques and show significant improvement compared to directly applying the local methods to the original input space. Intuitively, GSA based preprocessing handles global trends, and frees the local models to better represent nearby information. We formalize this intuition in Section 3.2 by proposing that the relationship between the warped inputs and the outputs be equally sensitive to every input dimension at the global level. We find that this can result in significant improvement in predictive ability on a battery of test functions and datasets.

This prewarping idea may be compared to the concept of preconditioning in numerical analysis (88). A central problem in numerical analysis is the solution of linear systems $\mathbf{Ax} = \mathbf{b}$, and modern solution algorithms are typically iterative, meaning that they operate by improving a given approximate solution $\tilde{\mathbf{x}}$ over the course of many iterations until the error $\|\mathbf{A}\tilde{\mathbf{x}} - \mathbf{b}\|$ is acceptable. Numerical analysts have found that oftentimes, by first performing a linear transformation to the input space, they improve the conditioning of the linear system which results in fewer iterations required for a given level of accuracy. Similarly, we propose performing a linear transformation of the input space based on a GSA in the hope that this will result in fewer *data* requirements for a given level of accuracy, or greater accuracy given data. If a surrogate prior to the linear transformation corresponds to fitting y_i versus \mathbf{x}_i , afterwards the problem becomes y_i versus \mathbf{Lx}_i , where \mathbf{L} is derived from an appropriate GSA.

In particular, given a large collection of simulator inputs \mathbf{X} and outputs \mathbf{y} , we propose first conducting a sensitivity analysis using a Gaussian Process (GP) fit to a (global) manageably-sized subset of the data. We prefer a separable kernel (details in Section 2) because learning correlation decay along each dimension is key to the fidelity of GSA. The Automatic Relevance Determination (ARD; 61, 68, Ch. 5.1) principle holds that those input dimensions with large kernel length-scales are less important, and can be dropped when conducting variable selection. Scaling each input dimension by the reciprocal of the associated length-scale, one possible \mathbf{L} , thus imbues the local surrogate with inductive bias reflecting global trends.

PCA is an option that goes beyond re-scaling to linear projection. However, PCA’s emphasis on dispersion means it’s less useful for surrogate modeling, where designs are typically chosen by the practitioner; i.e., no input dispersion to learn beyond that we have ourselves imposed. AS, however, allows for non-axis aligned measures of sensitivity, emitting an \mathbf{L} for the purposes of linear projection, while also accounting for the response. We provide the details of how such sensitivities may be realized through efficient sampling schemes, and how \mathbf{L} may be backed out for the purposes of input warping for downstream local analysis, and ultimately accurate prediction. We privilege ARD and AS \mathbf{L} prewarping, which we show both improve upon simple global and local schemes, however there are certainly other possibilities.

After reviewing relevant background in Section 2, our proposed methodology is detailed in Section 3. Section 4 begins by deploying our method on observational

data and low dimensional test functions, before tackling our motivating automotive example, a 124 dimensional problem with 500,000 observations. Section 5 concludes the article and overviews promising future work.

2. Background and Related Work

We review the gradient-based sensitivity analysis and pivot to GPs.

2.1. Gradient-Based Sensitivity Analysis

Several different approaches have been developed to formalize the notion of low intrinsic dimension of a black-box function $f : \mathbb{R}^m \rightarrow \mathbb{R}$, whose evaluations may require running an expensive computer simulation. This article is most concerned with methods that analyze the gradient of the target function, but it should be noted that other interesting approaches have been suggested, such as those based on characterizing the distribution of response given the important low dimensional subspace (17, 54) or based on variance (81). The relationship between gradient-based methods and variance-based methods is explored in (52).

If derivatives of the simulator are available with respect to input parameters, a natural way to define importance of the inputs is via the magnitude of $\frac{\partial f(\mathbf{x})}{\partial x_i}$ since this quantity tells us how much the output changes as the input variable i is perturbed.¹ However, gradients are a fundamentally local quantity, so are on their own ill-defined as a global sensitivity metric. Global analysis results from defining some manner of aggregating the function’s gradients throughout the input space. The techniques we review below, as well as those we deploy in our methodology, are defined as expectations of gradients over the input space, but it is worth noting that applications may motivate other approaches, for instance the maximum derivative $\max_{\mathbf{x} \in \mathcal{X}} |\frac{\partial f(\mathbf{x})}{\partial x_i}|$.

Sobol (80) proposed the quantity $\mathbb{E}\{(\frac{\partial f(\mathbf{x})}{\partial x_i})^2\}$ as a measure of variable importance for screening purposes, and described a Monte Carlo based estimator. Computing this estimate involves finite differencing, which may be infeasible for stochastic or numerically sensitive functions. To this end, (22) proposed GP-based estimates for derivatives. Since these screening methods entail retaining only inputs which have large derivatives, a natural extension is to consider directions within the input space which have large directional derivatives, effectively relaxing the constraint that these directions be aligned with the input axes. In this case, we are looking for linear combinations of input variables along which the function changes most drastically.

Functions which vary *only* in certain directions are called Ridge Functions, and are defined as functions of the form $f(\mathbf{x}) = g(\mathbf{A}\mathbf{x})$, where $\mathbf{A} \in \mathbb{R}^{r \times m}$ and g is any function on \mathbb{R}^r , and $r < m$. As a modeling device, ridge functions have inspired a number of

¹Note that this only makes sense if the input scales are comparable.

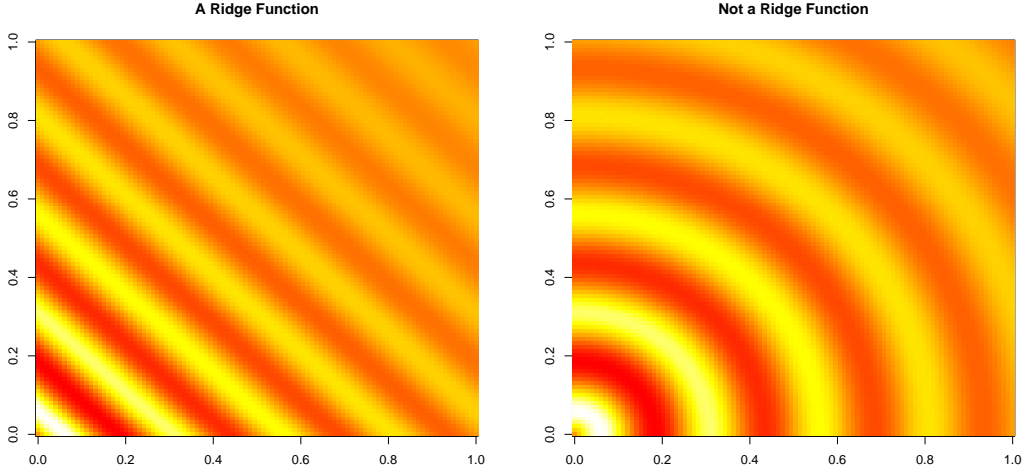


Figure 1. Heat plots of *left*: $f(z) = \sin(z) \cos(z)e^{-\frac{z}{10}}$, with $z = x + y$; and *right*: $z = \sqrt{x^2 + y^2}$.

nonlinear statistical predictors, including projection pursuit (31). In the ridge function framework, dimension reduction is assumed to be linear, but the actual function present on the low dimensional space need not be. The left panel of 1 shows the ridge function $f(x) = \sin(x + y) \cos(x + y)e^{-\frac{x+y}{10}}$. The eponymous ridges are visible as constant diagonal bands in the heat plot. Here, $\mathbf{A} = [1 \ 1]$, and $g(z) = \sin(z) \cos(z)e^{-\frac{z}{10}}$. Note, however, that ridge functions cannot exhibit “curvy” ridges, as in the right panel of the figure. From the ridge function perspective, the right image represents a two dimensional function, even if it depends only the one dimensional quantity $\sqrt{x^2 + y^2}$.

Active Subspace methods (15) provide a way to view functions as being “almost” ridge functions. This analysis considers the expected gradient outer product matrix

$$\mathbf{C} = \mathbb{E}_\nu \left[(\nabla f)(\nabla f)^\top \right] = \int (\nabla f)(\nabla f)^\top d\nu. \quad (1)$$

Functions are said to have an AS when they change *mostly* rather than uniquely along a small set of directions, formalized in the sense that \mathbf{C} has a gap in its eigenvalues. The eigenspace associated with the eigenvalues that make the cut are those directions in which large gradients are “often” pointed, relative to the measure ν .

In this article, the measure with respect to which the AS is defined will either be the Lebesgue measure ν_l or the sample probability measure ν_s , which is given by $\eta(\mathcal{A}) = \frac{1}{n}$ if $\mathcal{A} = \{\mathbf{x}_i\}$ for any sample point \mathbf{x}_i (such that taking the expectation of some quantity with respect to this measure is simply the average of that quantity observed at the sampling locations). We use ν to denote a generic probability measure.

The reader familiar with techniques such as PCA that analyze the spectrum of the *covariance* matrix might expect us instead to be interested in the quantity

$$\mathbb{E}_\nu \left[(\nabla f - \mathbb{E}_\nu [\nabla f])(\nabla f - \mathbb{E}_\nu [\nabla f])^\top \right] = \mathbb{E}_\nu \left[(\nabla f)(\nabla f)^\top \right] - \mathbb{E}_\nu [\nabla f] \mathbb{E}_\nu [\nabla f]^\top,$$

Analytically computing the integral defining \mathbf{C} is not possible for all but the simplest functions. However, if the gradient may be evaluated at arbitrary input locations, a Monte Carlo estimator may be formed by first sampling B many vectors $\mathbf{x}_i \sim \nu$, and then computing $\frac{1}{B} \sum_{i \in \{1, \dots, B\}} (\nabla f)(\mathbf{x}_i) (\nabla f)(\mathbf{x}_i)^\top$. As with the axis-aligned sensitivities, we can of course use finite-difference approximations when appropriate; Constantine (15) analyzes the effect of numerical error in this step on the quality of the overall estimate of \mathbf{C} . In situations where finite differencing is not appropriate, the derivative may again be estimated via nonparametric methods (64–66) and then plugged into the Monte Carlo estimator. Wycoff, et al. (91) showed that analytic integration over a GP surrogate for the black-box f , reviewed momentarily, is possible for common kernel functions combined with the measure ν_l .

The quantity \mathbf{C} has been studied in the context of observational data as early as (74). Kernel based estimates have been proposed in this context as well by (32) with respect to the sample measure ν_s , which was deployed by (56) to reduce the dimension of a Tsunami simulator. Authors have also considered second order derivatives. Li (55) proposes looking at Hessian eigen-decompositions in Principal Hessian Directions as well as a method to estimate the Hessian itself using Stein’s Lemma, effectively calculating the cross-covariance between the response and the outer product of the input vector. For more background on GSA, see (48).

2.2. Gaussian Processes

A stochastic process with index set \mathcal{X} is a rule for assigning to one or more elements of \mathcal{X} a joint distribution in a consistent manner. When these joint distributions are Gaussian, the rule must simply specify the mean vector and covariance matrix for any possible combination of inputs. In this article, we will restrict our attention to the case of $\mathcal{X} = [0, 1]^m$, which accommodates simulators represented as functions of m real-valued input parameters that are independently varied within certain bounds. In this case, the mean function is typically constant, $\mathbb{E}[y(\mathbf{X})] = \beta_0$, where $y(\mathbf{X})$ gives the random variables associated with the rows of \mathbf{X} , and β_0 are unknown parameters.

The covariance between any two of these vectors is often a simple function of some notion of distance between them. For instance, the popular Gaussian or squared exponential kernel is of the form

$$\text{Var}[y(\mathbf{x}_i), y(\mathbf{x}_j)] = \sigma^2 \exp \left\{ \frac{-\|\mathbf{x}_i - \mathbf{x}_j\|_2^2}{2l} \right\}, \quad (2)$$

where the length-scale parameter l controls how quickly correlation decays as the distance between the inputs increases, and the covariance parameter σ scales the correlation to turn it into a covariance. Broadly speaking, GP kernels differ firstly in how they calculate distance, and secondly in how that distance is translated into a covariance. Isotropic kernels such as (2) are those for which every input dimension is treated

identically in terms of distance calculations, whereas anisotropic kernels are free to violate this. For instance, a separable kernel assigns a different length-scale to each dimension, allowing for correlation to decay at different rates as different parameters are varied. Mathematically, this may be expressed as

$$k(\mathbf{x}_i, \mathbf{x}_j) := \text{Var}[y(\mathbf{x}_i), y(\mathbf{x}_j)] = \sigma^2 \exp \left\{ - \sum_{k=1}^m \frac{(x_{i,k} - x_{j,k})^2}{2l_k} \right\}, \quad (3)$$

as in the case of the so-called separable Gaussian kernel. Notice that each term in the sum in (3) has a different length-scale l_k in the denominator. Since as $l \rightarrow \infty$ the contribution of that dimension to the covariance matrix shrinks to zero, the Automatic Relevance Determination (ARD; 61, 68, Ch. 5.1) principle argues that dimensions with large length-scales can be ignored.² Operating somewhat along this principle, (50, 83) scale input dimensions according to the inverse of their length-scale before fitting models which involve finding local neighborhoods.

GPs have found success in many areas including spatial statistics, time series analysis and surrogate modeling (30, 40, 75). They serve as useful surrogates because they offer nonparametric flexibility while retaining the analytical tractability of much more restrictive models. Inference in a GP is typically conducted in a Bayesian manner. Training data, comprising observations $y(\mathbf{X})$ are collected at certain input locations \mathbf{X} and conditioned on, yielding a posterior GP with modified mean and covariance functions. The posterior mean and covariance can be evaluated at any desired point \mathbf{x}_{n+1} through textbook multivariate Gaussian conditioning:

$$\begin{aligned} y(\tilde{\mathbf{x}})|\mathbf{y}(\mathbf{X}) &\sim N(\mu_{n+1}, \Sigma_{n+1}) \\ \mu_{n+1} &= \beta_0 + k(\tilde{\mathbf{x}}, \mathbf{X})k(\mathbf{X}, \mathbf{X})^{-1}(\mathbf{y} - \beta_0) \\ \Sigma_{n+1} &= k(\tilde{\mathbf{x}}, \tilde{\mathbf{x}}) - k(\tilde{\mathbf{x}}, \mathbf{X})k(\mathbf{X}, \mathbf{X})^{-1}k(\mathbf{X}, \tilde{\mathbf{x}}) \end{aligned} \quad (4)$$

These formulas require the action of the inverse kernel matrix $k(\mathbf{X}, \mathbf{X})^{-1}$ on the predictive-training cross-covariance vector $k(\tilde{\mathbf{x}}, \mathbf{X})$. Inference for any unknown parameters θ , such as length-scales and level $\theta = (l, \beta_0)$, requires multivariate Gaussian density evaluations which additionally requires (log) determinants of $k(\mathbf{X}, \mathbf{X})$. The most straightforward way to obtain these quantities involves calculating the Cholesky decomposition of the kernel matrix, an operation which scales cubically with the number of training locations, n . This is computationally intractable when n approaches several thousand. Much recent work seeks to circumvent this bottleneck.

²Though, mathematically speaking, there is no guarantee that variable importance decreases monotonically with respect to its length-scale, see (91, Section 3.2) for a counterexample.

2.2.1. *Scaling Gaussian Processes to Many Observations*

Usually, an input point will only have high correlation with its neighbors, and negligible correlation with the majority of other points much farther away. However, this correlation will never quite fall to zero. Covariance tapering (33) involves smoothly nudging negligible correlations to zero, accommodating efficient sparse linear algebra.

Operating along similar lines, Local Approximate Gaussian Processes (laGP; 40, 41, Ch. 9.3), involve constructing a small model at prediction time, incorporating only training points near where a prediction is desired. These points may be selected via Nearest Neighbors (NN) or more sophisticated criteria. The Vecchia approximation (85) also exploits neighborhood structure, but this is used to build a partitioned likelihood, in effect asserting that only nearby points influence one another, similar to but distinct from covariance tapering. Originally introduced in the spatial statistics literature, the Vecchia approximation is most comfortable in low dimensional input spaces, which has motivated a thread of research to adapt it to higher dimensional problems such as surrogate modeling (50). That these models select a neighborhood set on the basis of inter-point distances means that proper prewarping could not only give the model a better perspective of inter-point distances within the set of local points itself, but also lead to a better set of local points.

Mercer’s Theorem tells us that kernel functions are associated with a mapping ψ from \mathcal{X} to a new space \mathcal{U} , in such a way that the inner product of the new features equals the Kernel matrix, $K_{i,j} = \langle \psi(\mathbf{x}_i), \psi(\mathbf{x}_j) \rangle$. For most popular kernels, this space is infinite dimensional. However, by explicitly choosing the space \mathcal{U} to be finite dimensional but sufficiently rich, the kernel matrix K has a rank bounded by the dimension of \mathcal{U} , and can be decomposed efficiently using Woodbury-style identities (and is invertible after adding the diagonal noise matrix). This is the thrust of Fixed Rank Kriging (19). Inducing Point Methods (68, 77, 78, Ch. 8) are another way of exploiting low rank structure. Instead of calculating the kernel applied to all $\mathcal{O}(n^2)$ pairs of points, the inner product is calculated between all training points and some smaller set of reference locations, knots, or so-called Inducing Points. Such low-rank methods are referred to as “sparse”, but in the sense of the covariance matrix’s spectrum, rather than entrywise sparsity, as is the case with covariance tapering.

The concern with large datasets may seem somewhat antithetical to the idea that each observation was obtained at great computational cost and should be optimally exploited. But in the context of complicated response surfaces, there is no choice but to perform the calculations for many input-output pairs. This is especially so for simulators with many inputs, as the cost of evaluating a space-filling design scales exponentially with dimension. Consequently, the adaptation of kernel-based surrogates to high dimensional problems is an area of active research.

2.2.2. *Scaling Gaussian processes to High Dimension*

There is nothing inherently problematic about GP modeling in high input dimension from a computational perspective, especially for simple isotropic kernels, because arithmetic operations scale cubically in n , not m . However, and especially without isotropy, one usually needs an exceedingly large design (large n) to create a rich enough training dataset in order to capture signal at high fidelity in that large input space. Thus, large input spaces tend to be linked to large training datasets. However, if one presumes that the intrinsic dimensionality is much lower than the nominal input dimension, one may be able to get away with a smaller training dataset if a mapping between input spaces can be learned. Consequently, many approaches for deploying GP as surrogates in high input dimension settings consist of building in dimensionality reduction. Perhaps the most straightforward way of conducting linear dimension reduction is to simply randomly choose the projection. This is the approach taken by Random Embeddings Bayesian Optimization (87, REMBO), and expanded upon in (5).

Beyond random projectors, many approaches have been suggested to find optimal projection matrices before fitting a GP on the reduced space. In the special case of a one-dimensional reduced space, Bayesian inference via Markov-Chain Monte Carlo has been proposed to learn the low dimensional subspace for both observational data (12) as well as for computer emulators (43) via Single-Index Models which build on the projection pursuit idea. Djolonga, et al. (25) combine finite differencing in random directions with a low rank matrix recovery algorithm to discover the projection matrix, and (34) give this approach a Bayesian treatment, even proposing an adaptive sampling algorithm to sequentially select informative design points. Where finite differencing is appropriate, Constantine, et al. (16) propose to deploy AS for selecting the low dimensional projection, and also discuss a heuristic for selecting kernel length-scale parameters on the reduced space.

Instead of defining the GP on a low dimensional space, alternatively, one could up the columns of the input space and define a model on each subdimensional part. For instance, (27, 29) propose Additive GPs, where the response is modeled as a sum of stochastic processes defined individually for each main effect. The sum can be expanded to include stochastic processes of any interaction level, as detailed in (28). Delbridge, et al. (24) lies at the intersection of random projection and additive kernels: several random projections are combined additively.

Thus far, we have only discussed linear projections. Several authors (79, 89) propose processing the input vectors through a neural network before comparison via a classical kernel function, and train the neural network by backpropagating through the GP.

3. Methodology

Our framework is in three parts: (1) sensitivity analysis to (2) define a warping of inputs, and (3) fitting local models in that space. These are discussed in turn.

3.1. *Global Sensitivity Analysis*

Section 2.1 presented several attractive methods for GSA, and indeed many others still could potentially be deployed in our framework. In this article, however, we will focus on three sensitivity analysis methods based on GP regression (Section 2.2). In most of our applications, the GP fits are derived from data subsets (tabled to Section 3.1.3), in order to keep computational costs manageable.

3.1.1. *Automatic Relevance Determination*

Typically viewed as a variable selection procedure rather than a sensitivity analysis method, ARD proceeds by fitting a GP with a separable kernel (3) and optimizing kernel hyperparameters with respect to the marginal likelihood. Once obtained, a “soft” ARD treats the estimated sensitivity of each input dimension as inversely proportional to the square root of the length-scale l_k . This is justified by an infinite length-scale $l_k \rightarrow \infty$ being equivalent to a model fit all but the k^{th} variable. In the truncation setting, the same argument justifies removing variables with large length-scales. As we will see in Section 3.2, the axis-aligned nature of ARD will result in axis-aligned warping of the original input space. AS has no such restriction.

3.1.2. *Active Subspaces*

Given a GP posterior with constant prior mean β_0 on f , a natural way to estimate \mathbf{C} is to use the posterior mean of the integral quantity it is defined by (Eq. 1), which is now a random variable as we are conducting Bayesian inference. Assuming a sufficiently smooth kernel function, the gradient vector at any point \mathbf{x}^* has a multivariate Gaussian posterior $\nabla f(\mathbf{x}^*) \sim N(\mu_{\nabla}, \Sigma_{\nabla})$, where

$$\begin{aligned} \mu_{\nabla} &= \mathbf{K}_{[\nabla, X]} \mathbf{K}_{[X, X]}^{-1} (\mathbf{y} - \beta_0), \\ \text{and } \Sigma_{\nabla} &= K_{[\nabla, \nabla]} - K_{[\nabla, X]} \mathbf{K}_{[X, X]}^{-1} K_{[X, \nabla]}. \end{aligned}$$

Above, $\mathbf{K}_{[\nabla, X]}$ represents the cross-covariance matrix between the gradient at \mathbf{x}^* and the observed outputs \mathbf{y} , and $\mathbf{K}_{[\nabla, \nabla]}$ represents the covariance matrix of the gradient vector. These quantities are easily derived in terms of derivatives of the kernel function

k (68, Ch. 9). We will use these facts to simplify the desired expectation:

$$\begin{aligned}\mathbb{E}_f[\mathbf{C}_\nu|\mathbf{y}] &= \mathbb{E}_f\left[\mathbb{E}_{\mathbf{x}\sim\nu}\left[(\nabla f)(\mathbf{x})(\nabla f(\mathbf{x})^\top)\mid\mathbf{y}\right]\right] \\ &= \mathbb{E}_{\mathbf{x}\sim\nu}\left[\mathbb{E}_f\left[(\nabla f)(\mathbf{x})(\nabla f(\mathbf{x})^\top)\mid\mathbf{y}\right]\right] = \mathbb{E}_{\mathbf{x}\sim\nu}\left[\Sigma_\nabla(\mathbf{x}) + \mu_\nabla(\mathbf{x})\mu_\nabla(\mathbf{x})^\top\right].\end{aligned}$$

For general ν , this expression may be evaluated via Monte Carlo. Wycoff, et al. (91) provided a closed form for when ν is the Lebesgue measure on $[0, 1]^m$ (denoted ν_l) and k is Gaussian (2–3) or Matérn with a smoothness parameter of $\nu = \frac{3}{2}$ or $\frac{5}{2}$.

The technique developed in (32) for kernel-based sensitivity analysis may be viewed as an AS estimator where ν is the sample measure ν_s , that is, the discrete distribution putting equal weight on encountered \mathbf{x} values, in which case

$$\mathbb{E}_f[\mathbf{C}_{\nu_s}|\mathbf{y}] = \frac{1}{n} \sum_{i=1}^n \Sigma_\nabla(\mathbf{x}_i) + \mu_\nabla(\mathbf{x}_i)\mu_\nabla(\mathbf{x}_i)^\top.$$

All of these quantities depend of course on our choice of kernel function k as well as its hyperparameters, which must be somehow estimated. In a typical GP framework, the marginal likelihood would be maximized. However, (32) bypass Gaussian assumptions. This is sensible as a sensitivity analysis should make as few assumptions as possible as it is itself meant to aide modeling and thus assumptions-making. Without a likelihood available, they recommend performing Cross Validation (CV) not over the GP itself, but instead over k -Nearest-Neighbors in the transformed space over a grid of hyperparameter values, while (56) set the values by trial and error. Due to the exponential growth of design points for fixed resolution, use of CV over a grid is restricted to low dimensional problems, which means that it is not appropriate for simultaneous selection of many kernel hyperparameters. This makes it unsuitable for kernels such as the separable Gaussian (Eq. 3), and consequently unsuitable for ARD. In estimating kernel hyperparameters via gradient based optimization of the marginal likelihood, we are able to deploy all of our sensitivity analyses from the same baseline.

3.1.3. Scaling Up

Since the downstream local emulation approaches (Section 3.3) scale to large datasets, we want to ensure that our method of preprocessing is scalable as well. Our GP estimates of the AS matrix and length-scales suffer the bottleneck of decomposing large covariance matrices, so a direct application is not feasible. Instead, we will employ a subbagging technique (8, 92). Given a number of subbags B and subbag size $n_B \ll n$, we sample B samples of size n_B , then calculate each of the B AS matrices \mathbf{C}_b as described in Section 3.1.2, before averaging them (See Algorithms 1–2). In the context of ARD, subsampling can be shown to provide consistent estimates of length-scale relative to MLEs estimated from the full data (57, 58). Extending to AS is natural,

but as yet unproven in practice. With an estimate of our sensitivity analysis in hand, we can go about exploiting it.

3.2. *Warping*

There are many ways one could use the sensitivity analysis we have just described to improve local models, depending of course on which analysis was conducted. Here we propose the heuristic of using the warping such that running the sensitivity analysis again afterwards would result in all directions being equally important. In the case of ARD, this would amount to conducting a warping such that the optimal length-scales are all equal to 1, while in the case of AS, this would be the case when $\mathbf{C} = \mathbf{I}$.

In both of these special cases the transformation is linear, and thus can be represented by a matrix \mathbf{L} . The matrix \mathbf{L} should premultiply each design point $\mathbf{z}_i = \mathbf{L}\mathbf{x}_i$, which looks like $\mathbf{Z} = \mathbf{X}\mathbf{L}^\top$ when the design points are stacked in the canonical design matrix $\mathbf{X} \in \mathbb{R}^{n \times m}$. This process may be seen as decomposing the black-box f into two parts: a linear transformation \mathbf{L} and a nonlinear function g . Here, g is the function upon which we are actually doing regression when we fit \mathbf{y} to \mathbf{Z} . We next will describe \mathbf{L} can be formed via ARD or AS sensitivity.

3.2.1. *Bandwidth Scaling*

When using the separable Gaussian kernel (Eq. 3), it is clear that using a length-scale of l_k for an input variable k living in $[0, 1]$ is equivalent to using a length-scale of $l_k = 1$ and a domain of $[0, \frac{1}{\sqrt{l_k}}]$. Therefore, scaling each input dimension by the root of its estimated length-scale would achieve our desired result. This is because fitting a GP to the scaled input-output relationship would result in length-scale estimates equal to 1 for all input variables.³

Algorithm 1 Bandwidth Scaling

Given: Data \mathbf{X}, \mathbf{y} , Bags B , Bag size n_{sub}

- 1: **for** $b \in \{1, \dots, B\}$ **do**
- 2: $\mathcal{I} \sim \text{Cat}\{1, \dots, N\}$ ▷ Subsampling
- 3: $\hat{\boldsymbol{\theta}}_b \leftarrow \underset{\boldsymbol{\theta}}{\text{argmin}} \mathcal{L}_{GP}(\mathbf{y}|\boldsymbol{\theta})$ ▷ Optimize GP Likelihood wrt $\boldsymbol{\theta}$
- 4: **end for**
- 5: $\hat{\boldsymbol{\theta}} \leftarrow \frac{1}{B} \sum_B \hat{\boldsymbol{\theta}}_B$
- 6: $\mathbf{L} \leftarrow \text{diag}(\hat{\boldsymbol{\theta}})$ ▷ Place Estimates in a Diagonal Matrix
- 7: $\mathbf{Z} \leftarrow \mathbf{X}\mathbf{L}^\top$

Since we are just scaling the input space, \mathbf{L} will be a diagonal matrix with nonzero

³Modulo numerical issues including finite precision and non-convexity.

elements given by the inverse root of the length-scales:

$$\mathbf{L}_{\text{ARD}} = \begin{bmatrix} \frac{1}{\sqrt{l_1}} & 0 & \dots & 0 \\ 0 & \frac{1}{\sqrt{l_2}} & \dots & 0 \\ \vdots & \vdots & \ddots & 0 \\ 0 & 0 & \dots & \frac{1}{\sqrt{l_m}} \end{bmatrix} \quad (5)$$

In (14, 40), this is treated as a preprocessing step, performed once before deployment within local models,⁴ while in (50) this scaling is iteratively updated as the marginal likelihood is optimized and the length-scale estimates change.

3.2.2. Active Subspace Rotation

In the case of a known AS matrix \mathbf{C} , the transformation \mathbf{L} which satisfies our desire to “undo” the sensitivity analysis is given by $\mathbf{L} = \Lambda^{1/2}\mathbf{U}^\top$, where $\mathbf{U} \in \mathbb{R}^{m \times m}$ is the matrix with columns giving the eigenvectors of \mathbf{C} and $\Lambda^{1/2}$ a diagonal matrix containing the square root of the eigenvalues. We will now show that this warping satisfies our heuristic. Recalling that $\nabla f(\mathbf{x}) = \nabla g(\mathbf{Lx}) = \mathbf{L}^\top \nabla g(\mathbf{Lx})$,

$$\begin{aligned} \mathbb{E}_\nu \left[(\nabla_x f(\mathbf{x}))(\nabla_x f(\mathbf{x}))^\top \right] &= \mathbb{E}_\nu \left[(\nabla_x g(\mathbf{Lx}))(\nabla_x g(\mathbf{Lx}))^\top \right] \\ \iff \mathbb{E}_\nu \left[(\nabla_x f(\mathbf{x}))(\nabla_x f(\mathbf{x}))^\top \right] &= \mathbb{E}_\nu \left[\mathbf{L}^\top (\nabla_{\mathbf{Lx}} g(\mathbf{Lx}))(\nabla_{\mathbf{Lx}} g(\mathbf{Lx}))^\top \mathbf{L} \right] \\ \iff \mathbb{E}_\nu \left[(\nabla_x f(\mathbf{x}))(\nabla_x f(\mathbf{x}))^\top \right] &= \mathbf{L}^\top \mathbb{E}_\nu \left[(\nabla_{\mathbf{Lx}} g(\mathbf{Lx}))(\nabla_{\mathbf{Lx}} g(\mathbf{Lx}))^\top \right] \mathbf{L} \\ \iff \mathbf{U}\Lambda\mathbf{U}^\top &= \mathbf{U}\Lambda^{\frac{1}{2}} \mathbb{E}_\nu \left[(\nabla_{\mathbf{Lx}} g(\mathbf{Lx}))(\nabla_{\mathbf{Lx}} g(\mathbf{Lx}))^\top \right] \Lambda^{\frac{1}{2}} \mathbf{U}^\top \\ \iff \Lambda &= \Lambda^{\frac{1}{2}} \mathbb{E}_\nu \left[(\nabla_{\mathbf{Lx}} g(\mathbf{Lx}))(\nabla_{\mathbf{Lx}} g(\mathbf{Lx}))^\top \right] \Lambda^{\frac{1}{2}} \\ \iff \mathbf{I} &= \mathbb{E}_\nu \left[(\nabla_{\mathbf{Lx}} g(\mathbf{Lx}))(\nabla_{\mathbf{Lx}} g(\mathbf{Lx}))^\top \right], \end{aligned}$$

or alternatively

$$\mathbb{E}_{\nu_{\mathbf{z}}} \left[(\nabla_{\mathbf{z}} g(\mathbf{z}))(\nabla_{\mathbf{z}} g(\mathbf{z}))^\top \right] = \mathbf{I}, \quad (6)$$

where $\nu_{\mathbf{z}}$ is the measure implied on $\mathbf{z} := \mathbf{Lx}$ by ν . Consequently, all directions are of equal import globally (at least up to the training data collected under the chosen experimental design), and the local model is freed to concentrate on local information. The decomposition is illustrated in Figure 2, which shows the trajectory from simulator input to simulator output in two different ways. The bottom of the figure shows the standard modeling approach, where the black-box simulator maps directly from the input space to the scalar response in an anisotropic manner. The top shows our proposed decomposition, where first a linear transformation maps the input hyper-

⁴Cole, et al., (14) attribute Bandwidth Scaling to Derek Bingham, who called it “stretching and compressing”.

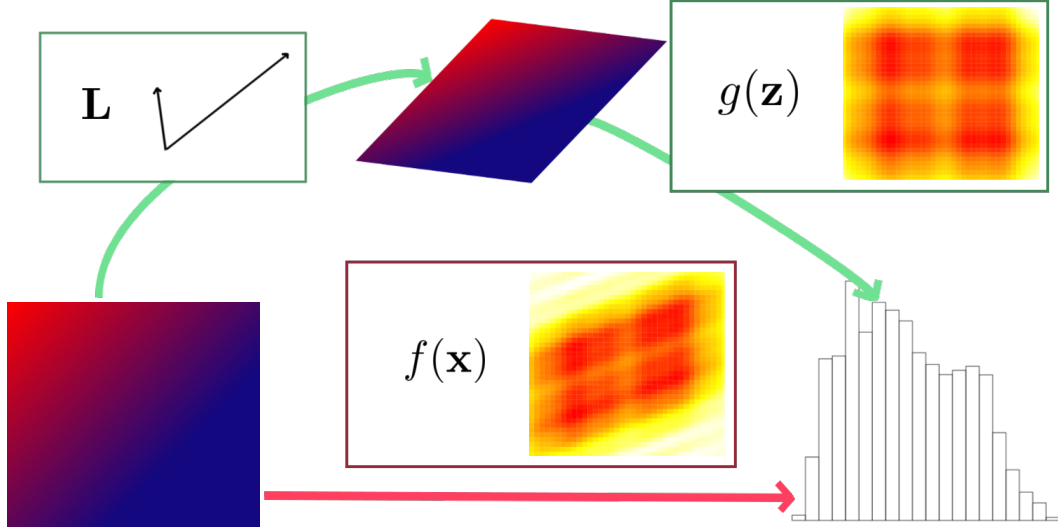


Figure 2. The function f (bottom, red line) with a nontrivial AS maps from $[0, 1]^2$ to \mathbb{R} . It may alternatively be viewed as a linear scaling $\mathbf{L} : [0, 1]^2 \rightarrow \mathbb{R}^2$, followed by a function g with all directions of equal importance (top, green lines). Before preprocessing, regression is on f ; afterwards on g .

cube into a polytope defined by the sensitivity analysis, and second the now isotropic nonlinear function may be modeled by local predictors. This procedure is delineated in Algorithm 2, which defines a family of warpings parameterized by the measure ν . In this article, we will study the transformations \mathbf{L}_l , associated with the Lebesgue measure, and \mathbf{L}_s , associated with the sample measure.

Algorithm 2 Active Subspace Rotation

- Given:** Data \mathbf{X}, \mathbf{y} , $\nu \in \{\text{Lebesgue, Sample}\}$, Bags B , Bag size nsub
- 1: **for** $b \in \{1, \dots, B\}$ **do** ▷ Subbagging Iteration
 - 2: $\mathcal{B} \sim \text{Cat}(\{1, \dots, N\}, \text{nsub})$ ▷ Subsampling
 - 3: $\hat{\theta}_B \leftarrow \underset{\theta}{\text{argmin}} \mathcal{L}_{GP}(\mathbf{y}_B, \mathbf{X}_B|\theta)$ ▷ Optimize GP Likelihood wrt θ
 - 4: $\hat{\mathbf{C}}_B \leftarrow \mathbb{E}_\nu [(\nabla f)(\mathbf{x})(\nabla f(\mathbf{x})^\top | \mathbf{y}_B)]$ ▷ Subset estimate of \mathbf{C}
 - 5: **end for**
 - 6: $\hat{\mathbf{C}} \leftarrow \frac{1}{B} \sum_B \hat{\mathbf{C}}_B$
 - 7: $\mathbf{U}, \Lambda \leftarrow \text{eigendecomp}(\hat{\mathbf{C}})$
 - 8: $\mathbf{L} \leftarrow \Lambda^{\frac{1}{2}} \mathbf{U}^\top$
 - 9: $\mathbf{Z} \leftarrow \mathbf{X}\mathbf{L}^\top$
-

3.2.3. Truncation

Once a transformation \mathbf{L} is calculated, we may additionally select a truncation dimension, creating another, more parsimonious class of options for the warping. That is, we entertain linear projections of lower rank. Determining the appropriate amount of such truncation depends on what local predictor is to be applied downstream, on the warped (and lower dimensional) inputs. We follow the approach outlined by (32),

which is actually designed to estimate kernel hyperparameters but it is easily adapted to any low-dimensional parameter, like model complexity. Our pseudo-code in that setting is provided in Algorithm 3. Notice that the method involves NN, however this is just one of many possible downstream models, a discussion we shall table for the moment. We take the same approach to truncation regardless of which GSA method gave rise to \mathbf{L} . In particular, NN is applied to each candidate dimension, and the sum of squared residuals computed. Rather than simply choosing that dimension which minimized error magnitude, we found that optimizing the Bayesian Information Criterion (BIC) was superior.⁵

Algorithm 3 Dimension Selection

Given: Rotated Design Matrix \mathbf{Z} , search interval $[\text{MIND}, \text{MAXD}]$.

- 1: **for** $r^* \in \{\text{MIND}, \dots, \text{MAXD}\}$ **do**
- 2: $\mathbf{Z}_{r^*} \leftarrow \mathbf{Z}[1 : r^*]$
- 3: $\text{mse}[r^*] \leftarrow \text{mean}(\text{KNN}(\mathbf{Z}_{r^*}, \mathbf{y})\$resid^2)$ $\triangleright k$ -Nearest Neighbors
- 4: $\text{bic}[r^*] \leftarrow n \log(\text{mse}[r^*]) + r^* \log(n)$
- 5: **end for**
- 6: $r \leftarrow \underset{\text{MIND} \leq r^* \leq \text{MAXD}}{\text{argmin}} \text{bic}[r^*]$

Arguably, this approach is somewhat mismatched if the downstream local predictor is not based on NN. And, indeed, if the practitioner is entering the modeling process with a particular local model in mind – our preferred options are enumerated next in Section 3.3 – it would be perfectly reasonable to select the truncation dimension via CV applied directly to that model. However, this would entail additional computational overhead, as NN is about as simple as it gets, and would also mean that the dimension needs to be reselected if a different local modeling approach is desired. In our experiments (Section 4), all of our local models use the same truncated dimension size r selected by Algorithm 3. Other approaches still are certainly possible. For instance, (15) suggests manual examination of \mathbf{C} 's spectrum for a gap, though such human intervention may be at odds with the otherwise hands-off, automated approach implied by the surrogate modeling context.

It is important to ensure that \mathbf{L} is properly ordered before we do truncation, to ensure that we are ignoring the least important directions when taking only the first r columns of \mathbf{Z} . For Bandwidth Scaling, this implies sorting the length-scales in increasing order (or the inverse-roots in decreasing order) along the diagonal of \mathbf{L} , while for AS prewarping, this involves making sure the elements of Λ and \mathbf{U} correspond to eigenpairs in decreasing order. This way, we make sure to drop the variables with the $m - r$ largest length-scales for \mathbf{L}_{ARD} , and those directions associated with the $m - r$ smallest eigenvalues for \mathbf{L}_l and \mathbf{L}_s .

⁵We treated the dimension of the NN model as the number of parameters it had and endowed it with a Gaussian error structure.

3.3. *Local Modeling*

For some regression methods, such as the basic linear model, linear transformations such as those we have described in this section so far would have no nontrivial impact. However, this is certainly not the case for local models, who are influenced in two major ways, namely by altering the partitioning scheme and by changing the default distance metric. Before we see exactly how, we provide an overview of the particular local models we prefer; Appendix A gives further algorithmic details and settings.

The simplest of these NN. To predict at $\tilde{\mathbf{x}}$, NN determines the k closest training locations to $\tilde{\mathbf{x}}$, then averages their responses to obtain a prediction. It is thus affected by the linear warping through the definition of “closest” changing, which thus alters the points which are being averaged for each prediction.

The laGP method also operates by building a prediction set at $\tilde{\mathbf{x}}$. And, just like NN, it begins with some number k of nearest neighbors to $\tilde{\mathbf{x}}$. Next, however, points are added to that set based on how useful they will be for prediction as measured by an acquisition criterion built on a GP. This GP is grown until some pre-specified “max” size. Just as with NN, the initial conditioning set will be influenced by the linear warping, but will further be affected through the change in distance metric used in its kernel function. This influences GP sequential neighborhood building as well as the predictions given the final “local dataset”.

The Vecchia approximation is a related but distinct idea. Unlike NN or laGP, which create local models at prediction time, the Vecchia approximation specifies a single generative story for the data. Each datapoint, rather than being conditioned upon all other training data, is instead conditioned in a cascade only on subsets and assumed conditionally independent of all others. However, this technique relies on the data being in some order, making the assumption that any data point is conditionally independent of all those data that come after it in the order given to those points in its conditioning set, which are constrained to come before. In Euclidean spaces of dimension greater than 1, there is no canonical ordering to turn to, so in practice an order is imposed on the data. This can be as simple as choosing to sort along whichever axis is perceived to be of greatest importance. In this article, we instead use the maximin ordering proposed by (44), which aims to minimize the discrepancy between points as inferred by the ordering as measured in Euclidean space. The Vecchia approximation stands to benefit from an improved ordering on top of neighborhood selection and distance metric change when prewarping is applied to it.

Illustrating Influence on Neighborhood Selection

We will now graphically explore the effect preprocessing can have on the sets of nearest neighbors. Specifically, points which are farther from the prediction location along axes with little influence, but closer along axes with much influence, are comparatively favored. Figure 3 illustrates this principle, revisiting the ridge function of Figure 1.

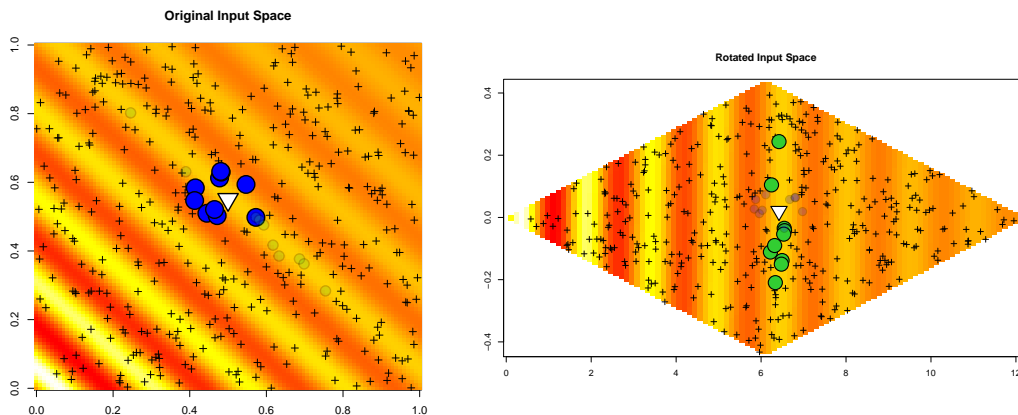


Figure 3. The function $f(x) = \sin(x + y) \cos(x + y) e^{-\frac{|x+y|}{10}}$ with x, y varying from -2π to 2π rescaled to $[0, 1]$, before (left) and after (right) \mathbf{L}_{ν_l} rotation. In both panels, the black + represent the training set and solid circles represent the 10 nearest neighbors to an arbitrary prediction location, itself represented by the large white triangle. Note that the rotated plot is not to scale for ease of viewing.

In this toy example, we sample 400 input locations uniformly at random in the 2d input domain, then applied Lebesgue-measure prewarping. The left panel shows the original input space, while the right plot shows the new input space after applying a \mathbf{L}_l rotation. The training set (black +’s) and prediction location (white triangle) are the same in both, but the nearest neighbors (green open circles) are changed. In each panel, the faded circles give the locations of the solid circles from the other plot. We can see that the response value at the ten nearest neighbors is much closer to the value at the predictive location after the warping (right) than it is before (left). If the next step after preprocessing were to conduct NN prediction, we can visually verify that the prediction after rotation will be more accurate than without.

4. Numerical Experiments

We shall now present results of experiments devised to quantitatively evaluate sensitivity prewarping in predictive exercises. We begin with outlining the comparators and metrics, followed by implementation details, and the actual experiments. R scripts reproducing all figures shown in this document are available at the link below.

<https://github.com/NathanWycoff/SensitivityPrewarping>

4.1. Implementation details, comparators and metrics

The preprocessing methods will be assessed based on their effect on the performance of downstream local models. As baselines, we entertain GPs fit on random data subsets, which we’ll denote **sGP**, as well as k -NN (**KNN**), laGP (**laGP**), and the Vecchia approximation (**vecc**) on the full, original dataset. Implementations are provided by R packages **hetGP** (6, 7), **FNN** (4), **laGP** (39, 41), and **GpGp** (44, 45), respectively.

These will be compared to `KNN`, `laGP` and `vecc` with the three specific prewarping methods we proposed in Section 3.2. The Bandwidth Scaling `LARD` will be denoted by the prefix `B`, Lebesgue-measure prewarping `Ll` by the prefix `L`, and sample-measure prewarping `Ls` by the prefix `S`. Further, we will consider truncation for all three prewarping techniques which is denoted by a postfix of `T`. Thus, `S-laGP` represents the performance of fitting an `laGP` model using Algorithm 2 with the sample measure but without any truncation (as that would be represented by `S-laGP-T`).

For each test function, we first generate data using either a random Latin Hypercube Sample (LHS; 82) via the R package `lhs` (10) for synthetic data, or via uniform random subsampling with existing/observational data, which we then randomly split into a train set and a test set. Then, we fit the baseline models for \mathbf{y} given \mathbf{X} and calculated their performance. Next, we conducted the sensitivity analyses using 5 subsamples each of size 1,500 in all experiments, using GP regression via the R package `hetGP` (6, 7), estimating kernel hyperparameters, as well as the nugget term, via MLE (42). Afterwards, we compute the associated transformations to warp each \mathbf{X} , yielding each \mathbf{Z} , as outlined in Algorithms 1 and 2. Finally, each local model is fit to \mathbf{Z} versus \mathbf{y} for each \mathbf{Z} created by the different transformations, and their performance on each recorded. This process was repeated for 10 Monte Carlo iterations.

In surrogate modeling, quantification of uncertainty is often high priority, so we define performance using not only the Mean Square prediction Error (MSE), but also logarithmic Score (36). For GP predictors, this is defined as the log likelihood of the response at a prediction location given the predictive mean and variance at that point using our assumption of Gaussianity for the response (36, Eq. 25). Since NN is typically not deployed in situations where uncertainty quantification is desired, we omit score calculations for it.

While calculation of \mathbf{C} can involve sophisticated machinery, deploying the proposed methodology in workflows based on R has been made as simple as possible. With the R package `activegp` (90, 91) loaded, prewarping is as straightforward as:

```
R> Lt <- Lt_GP(X, y, measure = "lebesgue")
R> Z <- X %*% Lt[,1:r]
```

where of course "lebesgue" may be replaced by "sample" and `r` gives the number of dimensions to retain, following Algorithm 3.

4.2. Observational Data

We first consider two high dimensional observational datasets. The Communities and Crime dataset⁶ combines census and law enforcement statistics from the United States. The task is to predict crime rate per capita given 122 socio-economic indicators measured on 1,994 individuals. The Temperature dataset⁷ involves temperature forecasting

⁶See (69); retrieved from <https://archive.ics.uci.edu/ml/datasets/communities+and+crime>

⁷See (11); retrieved from <http://theoval.cmp.uea.ac.uk/~gcc/competition/>

given the output of a weather model, and consists of 7117 observations and 106 features output by the weather model. `vecc` ran into numerical issues when fit directly on the high dimensional space, so we have retained only truncated versions of it.

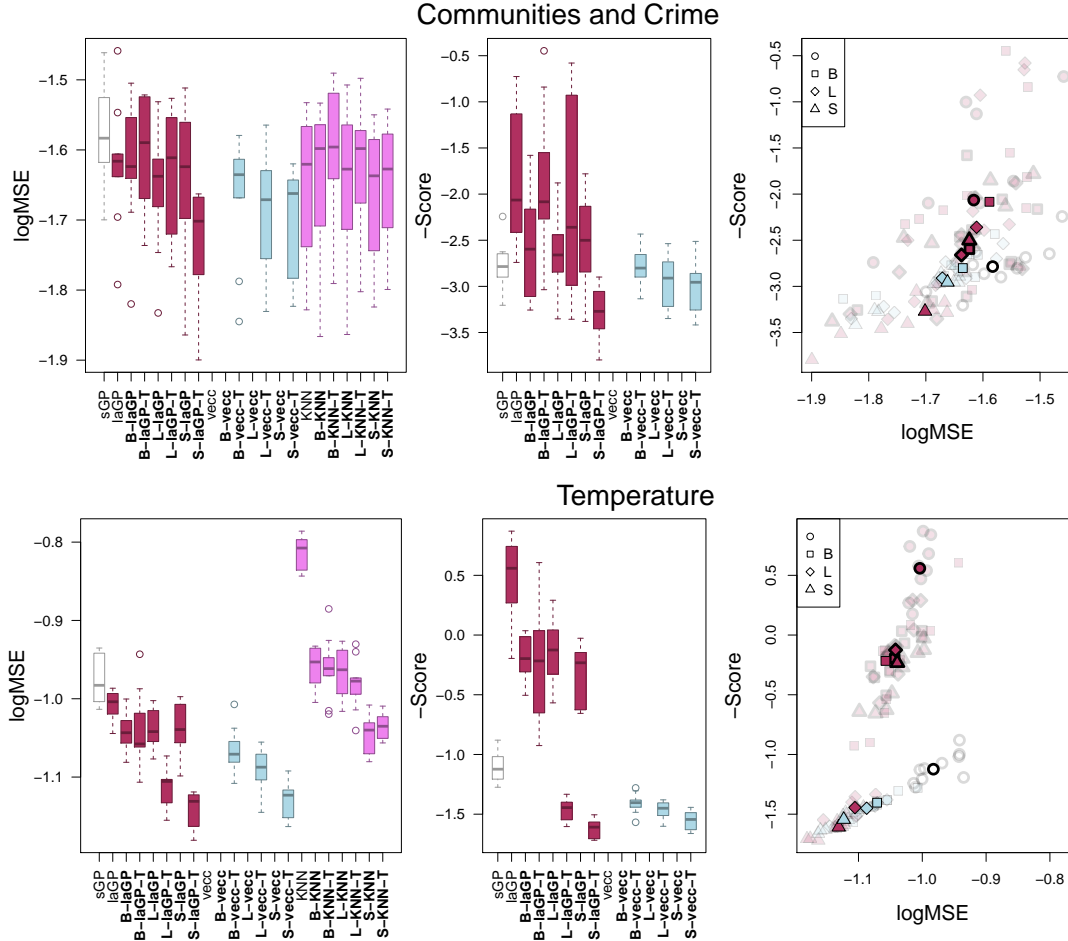


Figure 4. Results of simulations on two observational test problems in high dimension. *Left and Center:* the y -axis gives either \log_{10} MSE or negative Score (smaller is better). The letter before the name, B, L and S represents the transformation used for prewarping (if there is one), while presence of a T denotes truncation. **Bold** names indicate prewarping. Models that failed to fit are left blank. *Right:* \log_{10} MSE vs $-$ Score for each run; faded icons indicated individual run while solid icons give group medians. Circles indicate no prewarping, solid borders indicate no truncation.

The performance of the competing methods is given in Figure 4. We find that truncation is helpful for high dimensional problems, particularly on the Temperature dataset. We also find that the L_s generally outperforms L_l . This is because the observational data are not uniformly distributed, which has two implications. First, since the training set is not uniformly distributed, the Sample measure overemphasizes certain parts of the input space compared to the Lebesgue measure. Second, because the test set was formed by random sampling, these same parts of the input space that we have implicitly tuned our L estimate to are those parts of the input space in which we tend to find testing locations. In other words, there is simply a mismatch between the probability distribution from which the observational data were drawn and that

with respect to which \mathbf{L}_l is defined. We see that the preprocessing differentiated itself the least on the Communities and Crime problem, potentially because this problem consisted of significantly fewer observations, at around 1,000, making it difficult to estimate the rotation, and leading to high variance.

4.3. *Benchmark Test Functions*

We next evaluated the proposed methodology on benchmark test functions,⁸ where we found that prewarping increased performance in terms of both MSE and Score. In particular, we ran the competing methods on the Borehole ($46, m = 8$), Robot Arm ($1, m = 8$), and Piston ($51, m = 7$) functions with a training set size of 40,000 and test set size of 2,000 for each, sampled from a random LHS.

The result, shown in Figure 5, indicate that prewarping can be quite beneficial for local modeling in terms of predictive accuracy. On these low dimensional problems, each method performed similarly regardless of whether truncation was applied, so we have omitted truncation in the results. On all three problems, all forms of prewarping greatly outperform respective baselines. On the Borehole problem the AS based methods \mathbf{L}_l and \mathbf{L}_s outperform both the baselines and \mathbf{L}_{ARD} in terms of both MSE and Score. On the Robot Arm function, we find that all prewarping methods are pretty similar, with the sample-measure \mathbf{L}_s generally having a slight edge. Finally, on the Piston problem, prewarping generally leads to a decrease in MSE, though which particular method is ahead depends on the local model considered. In terms of Score, \mathbf{L}_s achieves the best result for both `laGP` and `vecc`.

4.4. *The MOPTA Problem*

In this section, we study the performance of prewarping on the mass optimization problem presented by General Motors at the 2008 Modeling and Optimization: Theory and Applications (MOPTA) conference (49). This problem concerns product design via computer experiments, in particular automotive design. The input variables characterize the design of the automobile, such as materials, part gauges, and shape, which determine the results of several crash simulations. The problem is to minimize the mass of the configuration, while observing constraints, such as the durability of the vehicle and the harshness of the crash. This is a constrained optimization problem involving 124 input variables and 68 constraints.⁹ While the standard approaches to smooth, high dimensional, constrained optimization are primarily gradient-based, the simulator, a multi-disciplinary effort, does not provide gradients with respect to inputs, and numerical noise means finite differencing approaches are not applicable.

Various authors have proposed sophisticated solutions for this challenging problem,

⁸See (84); retrieved from <https://www.sfu.ca/ssurjano/>

⁹FORTRAN code for this simulator was retrieved from <https://www.miguelanjos.com/jones-benchmark>

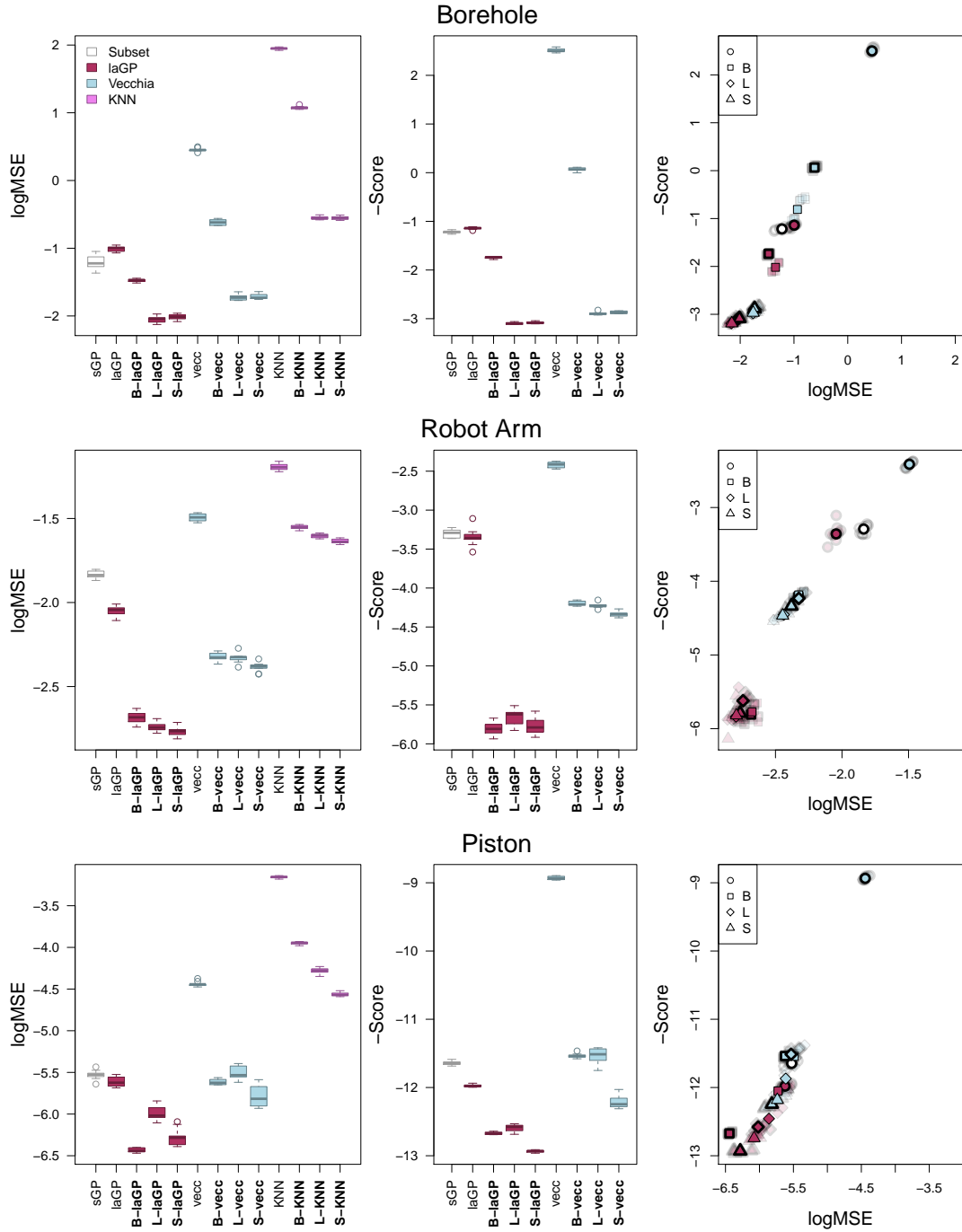


Figure 5. A comparison on common test functions with $n = 40,000$ runs. *Left and Center:* the y -axis gives either \log_{10} MSE or negative Score (smaller is better). **Bold** names indicate prewarping. The letter before the name, B, L and S represents the transformation used for prewarping (if there is one), while presence of a T denotes truncation. Each boxplot represents 10 runs with different design points. *Right:* \log_{10} MSE vs $-$ Score for each run; faded icons indicated individual run while solid icons give group medians. Circles indicate no prewarping, solid borders indicate no truncation.

including those based on Bayesian optimization, evolutionary strategies, or both. (70) proposed fitting a surrogate model to each constraint as well as the objective function to launch a stochastic search for good feasible solutions. (2) tackled the optimization

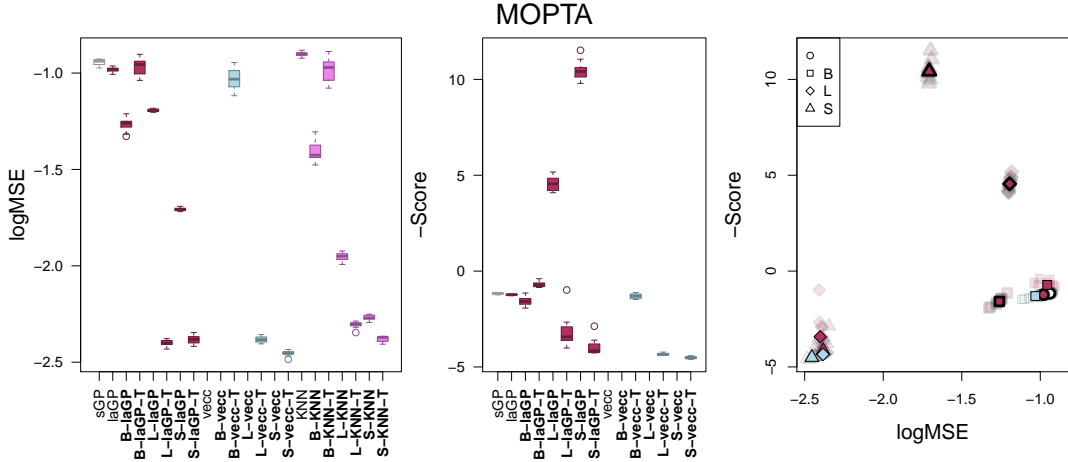


Figure 6. A comparison on the 124d MOPTA function. *Left and Center:* the y -axis gives either \log_{10} MSE or negative Score (smaller is better). The letter before the name, **B**, **L** and **S** represents the transformation used for prewarping (if there is one), while presence of a **T** denotes truncation. **Bold** labels indicate prewarping. Models that failed to fit left blank. *Right:* \log_{10} MSE vs $-$ Score for each run; faded icons indicated individual run while solid icons give group medians. Circles indicate no prewarping, solid borders indicate no truncation.

problem by effectively using an ensemble of surrogates, while (71) combined surrogate modeling approaches with evolutionary algorithms, and (72) combined surrogate modeling with trust region methods. However, this article is concerned with the large data regime, which is generally not the case when conducting Bayesian optimization. To study MOPTA as an emulation problem, we simply treat the sum of the objective and all of the constraints as a black-box function to approximate. This black-box is of interest as such augmented objective functions form the basis of penalty-based approaches to constrained optimization (62).

We sampled 500,000 points uniformly at random in the input space, treating 2,000 as a test set, chosen randomly. As before, `vecc` ran into numerical issues in high dimension and is only deployed in truncated input spaces. As the results in Figure 6 show, in terms of MSE, the prewarping without truncation can somewhat improve performance, but throwing in truncation as well results in improvements of an order of magnitude or more using doing AS prewarping (L_s or L_t). The exception is **S-KNN**, which is able to achieve competitive accuracy without truncation. In terms of score, it would appear that prewarping without truncation can result in a significant decrease in performance compared to baseline. Indeed, looking at the scatterplot (Figure 6, right), we see that without truncation, the various local models and prewarps form a spectrum of solutions trading MSE for Score, whereas the truncated AS prewarped local models significantly outperforms in terms of both. Notably, which prewarping is used has significantly greater impact than which local model is used.

5. Conclusions and Future Work

We introduced Sensitivity Prewarping, a simple-to-deploy framework for local surrogate modeling of computer experiments. Specifically, we proposed the heuristic of warping the space such that a global sensitivity analysis would reveal that all directions are equally important, and showed specific algorithms based on the ARD principle and/or AS to achieve this. By learning directions of global importance, we free each of the local models from individually learning global trends, and instead allow them to focus on their prediction region. Our prewarping effectively defines a new notion of distance which has the dual benefit of improving both neighborhood selection and the value of distance in prediction. We also proposed a subbagging procedure for scaling up inference of the AS as estimated via a GP.

Generally, our numerical experiments revealed that prewarping yields significant benefits in terms of predictive accuracy, as measured by MSE, as well as predictive uncertainty, as measured by Score. We showed how rotations can improve inference on low dimensional test functions, and how truncation can be transformative in high dimensional problems. Given the ease of implementation and the important improvement in predictive accuracy, we submit that this procedure has broad applicability.

In this article, we focused on three specific sensitivity analyses and three specific local models, but there is much more room for experimentation. In particular, we believe deploying this framework with nonlinear sensitivity analysis (i.e., that which can measure the importance of nonlinear functions of the inputs) could be fruitful, for instance Active Manifolds (9). It would also be interesting to study what sensitivity techniques could be expected to perform well when paired with a given local model.

Another area where future work could lend improvements is in large scale estimation of \mathbf{C} . In this article, we proposed a subbagging solution, but many other approaches are conceivable. For instance, \mathbf{C} could be computed by using existing approximations to the kernel matrix, such as the Vecchia approximation. An alternative would be to deploy Krylov subspace methods, which have shown great promise in scaling GPs (26, 35, 67, 86), to develop stochastic algorithms either to estimate the matrix \mathbf{C} itself or its leading eigenspace directly (37).

Arguably, the weakest link of this approach is the GP fit in the first stage which produces our estimator of \mathbf{C} , required to compute \mathbf{L} in the AS approach. This is because local models can compensate for breaches of our GP assumptions such as stationarity and homoskedasticity, while the global fit cannot. Hence, designing techniques for estimation of \mathbf{C} via more sophisticated models is likely to be a fruitful thread of research. Deep GPs (21) are a natural next step, and have been recently studied in the context of computer experiments (76). Finally, the simulators we studied in this article all accepted a vector of inputs and returned a scalar response. However, this is certainly not always the case: extensions to vector-valued, discrete, or functional responses would increase the breadth of problems this framework can take on.

References

- (1) Jian An and Art Owen. Quasi-regression. *Journal of Complexity*, 17(4):588 – 607, 2001.
- (2) P. Beaucaire, Charlotte Beauthier, and Caroline Sainvitu. Multi-point infill sampling strategies exploiting multiple surrogate models. pages 1559–1567, 07 2019.
- (3) Alexandre Belloni, Victor Chernozhukov, and Christian Hansen. Inference on Treatment Effects after Selection among High-Dimensional Controls†. *The Review of Economic Studies*, 81(2):608–650, 11 2013.
- (4) Alina Beygelzimer, Sham Kakadet, John Langford, Sunil Arya, David Mount, and Shengqiao Li. *FNN: Fast Nearest Neighbor Search Algorithms and Applications*, 2013. R package version 1.1.
- (5) Mickaël Binois, David Ginsbourger, and Olivier Roustant. A warped kernel improving robustness in bayesian optimization via random embeddings. In *International Conference on Learning and Intelligent Optimization*, pages 281–286. Springer, 2015.
- (6) Mickael Binois and Robert B. Gramacy. *hetGP: Heteroskedastic Gaussian Process Modeling and Design under Replication*, 2019. R package version 1.1.2.
- (7) Mickaël Binois, Robert B. Gramacy, and Mike Ludkovski. Practical heteroscedastic gaussian process modeling for large simulation experiments. *Journal of Computational and Graphical Statistics*, 27(4):808–821, 2018.
- (8) Leo Breiman. Bagging predictors. *Machine Learning*, 24(2):123–140, Aug 1996.
- (9) Robert A Bridges, Anthony D Gruber, Christopher Felder, Miki Verma, and Chelsey Hoff. Active manifolds: A non-linear analogue to active subspaces. *arXiv preprint arXiv:1904.13386*, 2019.
- (10) Rob Carnell. *lhs: Latin Hypercube Samples*, 2020. R package version 1.0.2.
- (11) G. C. Cawley, M. R. Haylock, and S. R. Dorling. Predictive uncertainty in environmental modelling. In *The 2006 IEEE International Joint Conference on Neural Network Proceedings*, pages 5347–5354, 2006.
- (12) Taeryon Choi, Jian Q. Shi, and Bo Wang. A Gaussian process regression approach to a single-index model. *Journal of Nonparametric Statistics*, 23(1):21–36, 2011.
- (13) David Cohn. Neural network exploration using optimal experiment design. In J. Cowan, G. Tesauro, and J. Alspector, editors, *Advances in Neural Information Processing Systems*, volume 6, pages 679–686. Morgan-Kaufmann, 1994.
- (14) D. Austin Cole, Ryan Christianson, and Robert B. Gramacy. Locally induced Gaussian processes for large-scale simulation experiments, 2020.
- (15) Paul G. Constantine. *Active Subspaces*. SIAM, Philadelphia, PA, 2015.
- (16) Paul G. Constantine, Eric Dow, and Qiqi Wang. Active subspace methods in theory and practice: Applications to kriging surfaces. *SIAM Journal on Scientific Computing*, 36(4):A1500–A1524, 2014.
- (17) R. Dennis Cook and Sanford Weisberg. Sliced inverse regression for dimension reduction: Comment. *Journal of the American Statistical Association*, 86(414):328–332, 1991.
- (18) Giovanni G. Crema, Farnaz Ghazi Nezami, and Srinivas R. Chakravarthy. A stochastic model for managing an assemble-to-order system. In *Proceedings of the 2015 Winter Simulation Conference, WSC '15*, page 2283–2294. IEEE Press, 2015.
- (19) Noel Cressie and Gardar Johannesson. Fixed rank kriging for very large spatial data sets. *Journal of the Royal Statistical Society: Series B (Statistical Methodology)*, 70(1):209–226,

- 2008.
- (20) S Da Veiga, F Wahl, and F Gamboa. Local polynomial estimation for sensitivity analysis on models with correlated inputs. *Technometrics*, 51(4):452–463, 2009.
 - (21) Andreas Damianou and Neil Lawrence. Deep gaussian processes. In Carlos M. Carvalho and Pradeep Ravikumar, editors, *Proceedings of the Sixteenth International Conference on Artificial Intelligence and Statistics*, volume 31 of *Proceedings of Machine Learning Research*, pages 207–215, Scottsdale, Arizona, USA, 29 Apr–01 May 2013. PMLR.
 - (22) Matthias De Lozzo and Amandine Marrel. Estimation of the derivative-based global sensitivity measures using a Gaussian process metamodel. *SIAM/ASA Journal on Uncertainty Quantification*, 4(1):708–738, 2016.
 - (23) Juliana B. de Souza, Valdério A. Reisen, Glauro C. Franco, Márton Ispány, Pascal Bondon, and Jane Meri Santos. Generalized additive models with principal component analysis: an application to time series of respiratory disease and air pollution data. *Journal of the Royal Statistical Society: Series C (Applied Statistics)*, 67(2):453–480, 2018.
 - (24) Ian A Delbridge, David S Bindel, and Andrew Gordon Wilson. Randomly projected additive Gaussian processes for regression. *arXiv preprint arXiv:1912.12834*, 2019.
 - (25) Josip Djolonga, Andreas Krause, and Volkan Cevher. High-dimensional Gaussian process bandits. In *Advances in Neural Information Processing Systems 26*, pages 1025–1033, 2013.
 - (26) Kun Dong, David Eriksson, Hannes Nickisch, David Bindel, and Andrew Wilson. Scalable log determinants for Gaussian process kernel learning. In *Advances in Neural Information Processing Systems*, pages 6330–6340, 2017.
 - (27) Nicolas Durrande, David Ginsbourger, and Olivier Roustant. Additive kernels for Gaussian process modeling. *Annales de la Faculté de Sciences de Toulouse*, page 17, 2012.
 - (28) Nicolas Durrande, David Ginsbourger, Olivier Roustant, and Laurent Carraro. ANOVA kernels and RKHS of zero mean functions for model-based sensitivity analysis. *Journal of Multivariate Analysis*, 115:57–67, 2013.
 - (29) David K. Duvenaud, Hannes Nickisch, and Carl E. Rasmussen. Additive Gaussian processes. In J. Shawe-Taylor, R. S. Zemel, P. L. Bartlett, F. Pereira, and K. Q. Weinberger, editors, *Advances in Neural Information Processing Systems 24*, pages 226–234. Curran Associates, Inc., 2011.
 - (30) A. Forrester, A. Sobester, and A. Keane. *Engineering Design via Surrogate Modelling: A Practical Guide*. Wiley, 2008.
 - (31) Jerome H. Friedman and Werner Stuetzle. Projection pursuit regression. *Journal of the American Statistical Association*, 76(376):817–823, 1981.
 - (32) Kenji Fukumizu and Chenlei Leng. Gradient-based kernel dimension reduction for regression. *Journal of the American Statistical Association*, 109(505):359–370, 2014.
 - (33) Reinhard Furrer, Marc G Genton, and Douglas Nychka. Covariance tapering for interpolation of large spatial datasets. *Journal of Computational and Graphical Statistics*, 15(3):502–523, 2006.
 - (34) Roman Garnett, Michael A. Osborne, and Philipp Hennig. Active learning of linear embeddings for Gaussian processes. In *Proceedings of the Thirtieth Conference on Uncertainty in Artificial Intelligence*, UAI’14, pages 230–239. AUAI Press, 2014.
 - (35) Mark Gibbs and David J.C. MacKay. Efficient implementation of Gaussian processes.

- Technical report, 1997.
- (36) Tilmann Gneiting and Adrian E Raftery. Strictly proper scoring rules, prediction, and estimation. *Journal of the American Statistical Association*, 102(477):359–378, 2007.
 - (37) Gene H. Golub and Gérard Meurant. *Matrices, Moments and Quadrature with Applications*. Princeton University Press, 2010.
 - (38) RB Gramacy, MA Taddy, and SM Wild. Variable selection and sensitivity analysis using dynamic trees, with an application to computer code performance tuning. *The Annals of Applied Statistics*, 7(1):51–80, 2013.
 - (39) Robert B. Gramacy. laGP: Large-scale spatial modeling via local approximate Gaussian processes in R. *Journal of Statistical Software*, 72(1):1–46, 2016.
 - (40) Robert B. Gramacy. *Surrogates: Gaussian Process Modeling, Design and Optimization for the Applied Sciences*. Chapman Hall/CRC, Boca Raton, Florida, 2020. <http://bobby.gramacy.com/surrogates/>.
 - (41) Robert B. Gramacy and Daniel W. Apley. Local Gaussian process approximation for large computer experiments. *Journal of Computational and Graphical Statistics*, 24(2):561–578, 2015.
 - (42) Robert B. Gramacy and Herbert K. H. Lee. Cases for the nugget in modeling computer experiments. *Statistics and Computing*, 22(3):713–722, May 2012.
 - (43) Robert B. Gramacy and Heng Lian. Gaussian process single-index models as emulators for computer experiments. *Technometrics*, 54(1):30–41, 2012.
 - (44) Joseph Guinness. Permutation and grouping methods for sharpening Gaussian process approximations. *Technometrics*, 60(4):415–429, 2018. PMID: 31447491.
 - (45) Joseph Guinness, Matthias Katzfuss, and Youssef Fahmy. *GpGp: Fast Gaussian Process Computation Using Vecchia’s Approximation*, 2020. R package version 0.3.1.
 - (46) W. V. Harper and S. K. Gupta. Sensitivity/uncertainty analysis of a borehole scenario comparing latin hypercube sampling and deterministic sensitivity approaches. Technical report, Office of Nuclear Waste Isolation, 1983.
 - (47) Trevor Hastie, Robert Tibshirani, and Jerome Friedman. *The Elements of Statistical Learning*. Springer Series in Statistics. Springer New York Inc., New York, NY, USA, 2009.
 - (48) Bertrand Iooss and Paul Lemaître. A review on global sensitivity analysis methods. In C. Meloni and G. Dellino, editors, *Uncertainty Management in Simulation-Optimization of Complex Systems: Algorithms and Applications*, pages 101–122. Springer, 2015.
 - (49) Donald R Jones. Large-scale multi-disciplinary mass optimization in the auto industry.
 - (50) Matthias Katzfuss, Joseph Guinness, and Earl Lawrence. Scaled vecchia approximation for fast computer-model emulation, 2020.
 - (51) Ron Kenett and S. Zacks. *Modern Industrial Statistics: Design and Control of Quality and Reliability*. Duxbury Press, 1998.
 - (52) Sergey Kucherenko and Bertrand Iooss. *Derivative-Based Global Sensitivity Measures*, pages 1–24. Springer International Publishing, Cham, 2016.
 - (53) Bing Li, Hongyuan Zha, and Francesca Chiaromonte. Contour regression: A general approach to dimension reduction. *Ann. Statist.*, 33(4):1580–1616, 08 2005.
 - (54) Ker-Chau Li. Sliced inverse regression for dimension reduction. *Journal of the American Statistical Association*, 86(414):316–327, 1991.

- (55) Ker-Chau Li. On principal Hessian directions for data visualization and dimension reduction: Another application of Stein’s lemma. *Journal of the American Statistical Association*, 87(420):1025–1039, 1992.
- (56) Xiaoyu Liu and Serge Guillas. Dimension reduction for Gaussian process emulation: An application to the influence of bathymetry on tsunami heights. *SIAM/ASA Journal on Uncertainty Quantification*, 5(1):787–812, 2017.
- (57) Y. Liu and Y. Hung. Latin hypercube design-based block bootstrap for computer experiment modeling. Technical report, Rutgers, The State University of New Jersey, New Brunswick, New Jersey, 2015.
- (58) Yufan Liu. Recent advances in computer experiment modeling. Technical report, Rutgers, The State University of New Jersey, New Brunswick, New Jersey, 2014.
- (59) A Marrel, B Iooss, B Laurent, and O Roustant. Calculations of Sobol indices for the Gaussian process metamodel. *Reliability Engineering & System Safety*, 94(3):742–751, 2009.
- (60) G. Paul Montgomery and Lynn T. Truss. Combining a statistical design of experiments with formability simulations to predict the formability of pockets in sheet metal parts. In *SAE Technical Paper*. SAE International, 03 2001.
- (61) Radford M. Neal. *Bayesian Learning for Neural Networks*. Springer-Verlag, Berlin, Heidelberg, 1996.
- (62) Jorge Nocedal and Stephen J. Wright. *Numerical Optimization*. Springer, New York, NY, USA, second edition, 2006.
- (63) JE Oakley and A O’Hagan. Probabilistic sensitivity analysis of complex models: a Bayesian approach. *Journal of the Royal Statistical Society: Series B (Statistical Methodology)*, 66(3):751–769, 2004.
- (64) Carsten Othmer, Trent W. Lukaczyk, Paul Constantine, and Juan J. Alonso. On active subspaces in car aerodynamics. In *17th AIAA/ISSMO Multidisciplinary Analysis and Optimization Conference*. American Institute of Aeronautics and Astronautics, 2016.
- (65) Pramudita S Palar and Koji Shimoyama. On the accuracy of kriging model in active subspaces. In *2018 AIAA/ASCE/AHS/ASC Structures, Structural Dynamics, and Materials Conference*, page 0913, 2018.
- (66) Pramudita Satria Palar and Koji Shimoyama. Exploiting active subspaces in global optimization: How complex is your problem? In *Proceedings of the Genetic and Evolutionary Computation Conference Companion on - GECCO ’17*, pages 1487–1494. ACM Press, 2017.
- (67) Geoff Pleiss, Jacob Gardner, Kilian Weinberger, and Andrew Gordon Wilson. Constant-time predictive distributions for Gaussian processes. In Jennifer Dy and Andreas Krause, editors, *Proceedings of the 35th International Conference on Machine Learning*, volume 80 of *Proceedings of Machine Learning Research*, pages 4114–4123, Stockholmsmässan, Stockholm Sweden, 10–15 Jul 2018. PMLR.
- (68) Carl E. Rasmussen and Christopher Williams. *Gaussian Processes for Machine Learning*. MIT Press, 2006.
- (69) Michael Redmond and Alok Baveja. A data-driven software tool for enabling cooperative information sharing among police departments. *European Journal of Operational Research*, 141(3):660 – 678, 2002.

- (70) Rommel G. Regis. Stochastic radial basis function algorithms for large-scale optimization involving expensive black-box objective and constraint functions. *Computers and Operations Research*, 38(5):837 – 853, 2011.
- (71) Rommel G. Regis. Surrogate-assisted evolutionary programming for high dimensional constrained black-box optimization. In *Proceedings of the 14th Annual Conference Companion on Genetic and Evolutionary Computation*, GECCO '12, page 1431–1432, New York, NY, USA, 2012. Association for Computing Machinery.
- (72) Rommel G. Regis and Stefan M. Wild. Conorbit: constrained optimization by radial basis function interpolation in trust regions. *Optimization Methods and Software*, 32(3):552–580, 2017.
- (73) J. J. Rodriguez, L. I. Kuncheva, and C. J. Alonso. Rotation forest: A new classifier ensemble method. *IEEE Transactions on Pattern Analysis and Machine Intelligence*, 28(10):1619–1630, 2006.
- (74) Alexander M. Samarov. Exploring regression structure using nonparametric functional estimation. *Journal of the American Statistical Association*, 88(423):836–847, 1993.
- (75) TJ Santner, BJ Williams, and W Notz. *The Design and Analysis of Computer Experiments, Second Edition*. Springer–Verlag, New York, NY, 2018.
- (76) Annie Sauer, Robert B. Gramacy, and David Higdon. Active learning for deep Gaussian process surrogates, 2020.
- (77) Alex Smola and Peter Bartlett. Sparse greedy Gaussian process regression. In T. Leen, T. Dietterich, and V. Tresp, editors, *Advances in Neural Information Processing Systems*, volume 13, pages 619–625. MIT Press, 2001.
- (78) Edward Snelson and Zoubin Ghahramani. Sparse Gaussian processes using pseudo-inputs. In Y. Weiss, B. Schölkopf, and J. Platt, editors, *Advances in Neural Information Processing Systems*, volume 18, pages 1257–1264. MIT Press, 2006.
- (79) Edward Snelson, Zoubin Ghahramani, and Carl Rasmussen. Warped Gaussian processes. In S. Thrun, L. Saul, and B. Schölkopf, editors, *Advances in Neural Information Processing Systems*, volume 16, pages 337–344. MIT Press, 2004.
- (80) I. Sobol and A Gersham. On an alternative global sensitivity estimator. *Proceedings of SAMO*, pages 40–42, 1995.
- (81) I.M Sobol. Global sensitivity indices for nonlinear mathematical models and their Monte Carlo estimates. *Mathematics and Computers in Simulation*, 55(1):271–280, 2001. The Second IMACS Seminar on Monte Carlo Methods.
- (82) Michael Stein. Large sample properties of simulations using latin hypercube sampling. *Technometrics*, 29(2):143–151, 1987.
- (83) F Sun, RB Gramacy, B Haaland, E Lawrence, and A Walker. Emulating satellite drag from large simulation experiments. *SIAM/ASA Journal on Uncertainty Quantification*, 7(2):720–759, 2019. preprint arXiv:1712.00182.
- (84) S. Surjanovic and D. Bingham. Virtual library of simulation experiments: Test functions and datasets. Retrieved December 10, 2020, from <http://www.sfu.ca/~ssurjano>.
- (85) A. V. Vecchia. A new method of prediction for spatial regression models with correlated errors. *Journal of the Royal Statistical Society. Series B (Methodological)*, 54(3):813–830, 1992.
- (86) Grace Wahba, Donald R. Johnson, Feng Gao, and Jianjian Gong. Adaptive tuning of

- numerical weather prediction models: Randomized gcw in three- and four-dimensional data assimilation. *Monthly Weather Review*, 123(11):3358 – 3370, 01 Nov. 1995.
- (87) Ziyu Wang, Frank Hutter, Masrour Zoghi, David Matheson, and Nando de Freitas. Bayesian optimization in a billion dimensions via random embeddings. *Journal of Artificial Intelligence Research*, 55:361–387, 2016.
- (88) A. J. Wathen. Preconditioning. *Acta Numerica*, 24:329–376, 2015.
- (89) Andrew Gordon Wilson, Zhiting Hu, Ruslan Salakhutdinov, and Eric P Xing. Deep kernel learning. In *Artificial intelligence and statistics*, pages 370–378, 2016.
- (90) Nathan Wycoff and Mickael Binois. *activegp: Gaussian Process Based Design and Analysis for the Active Subspace Method*, 2020. R package version 1.0.6.
- (91) Nathan Wycoff, Mickael Binois, and Stefan M. Wild. Sequential Learning of Active Subspaces. *arXiv e-prints*, page arXiv:1907.11572, July 2019.
- (92) Yibo Zhao, Yasuo Amemiya, and Ying Hung. Efficient gaussian process modeling using experimental design-based subbagging. *Statistica Sinica*, 28(3):1459–1479, 2018.
- (93) Huamin Zhou. *Computer Modeling for Injection Molding: Simulation, Optimization, and Control*, pages 25–47. 03 2013.

Appendix A. Local Model Details

KNN regression was implemented using the R package `FNN` (4); we used the default $K = 3$ with Euclidean distance for neighborhood selection. When using KNN to select what dimension to truncate to, all dimension values between 5 and 25 were evaluated.

`laGP` was implemented using the R package `laGP` (39). We used the default neighborhood selection procedure, which consists of choosing six nearest neighbors, then sequentially choosing new design points to add based on the Active Learning Cohn (ALC)(13) criterion. The point which optimizes ALC is that which the GP thinks will result in the greatest reduction in average predictive variance:

$$h_{\text{alc}}(\tilde{\mathbf{x}}) = \int_{\mathcal{X}} \text{Var} [y(\mathbf{x})|\mathbf{y}(\mathbf{X})] - \text{Var} [y(\mathbf{x})|\mathbf{y}(\mathbf{X}), y(\tilde{\mathbf{x}})] d\nu_l(\mathbf{x}). \quad (\text{A1})$$

The `laGP` model fit without prewarping uses a separable Gaussian kernel (Eq. 3), while those models fit after prewarping use an isotropic Gaussian kernel (Eq. 2). This was to allow the baseline model to discover some of the information the local model receives from the prewarping. Informal experiments revealed that changing acquisition criteria or neighborhood sizes did not qualitatively affect our conclusions. The procedure is outlined in Algorithm 4.

`Vecchia` was implemented using the R package `GpGp` (45). We used the default conditioning set sizes of 30 for optimizing kernel hyperparameters and 60 at prediction time, as well as the isotropic exponential covariance function, given by $k(y(\mathbf{x}_i), y(\mathbf{x}_j)) = \sigma^2 \exp\{-\frac{\|\mathbf{x}_i - \mathbf{x}_j\|_2}{2l}\}$, the difference from Equation 2 being that the distance in the numerator is not squared. We used the greedy maximin ordering(44),

Algorithm 4 Local Approximate Gaussian Process Regression

Given: Prediction location \mathbf{x}^* ; Neighborhood start size **start** and end size **end**;

- 1: $\mathbf{X}^* \leftarrow \text{NearestNeighbors}(\mathbf{x}^*, \mathbf{X}, \text{start})$ ▷ Nearest Neighbors init
- 2: **for** $i \in \{1, \dots, \text{end} - \text{start}\}$ **do** ▷ Sequential Neighborhood building
- 3: $\mathbf{x}^* \leftarrow \underset{\mathbf{x} \in \mathcal{X}}{\text{argmax}} h_{\text{ALC}}(\mathbf{x})$
- 4: $\mathbf{X}^* \leftarrow [\mathbf{X}^*, \mathbf{x}^*]$
- 5: **end for**
- 6: $\hat{y}(\mathbf{x}^*) = \text{GPpred}(\mathbf{x}, \mathbf{X}^*, \mathbf{y}(\mathbf{X}^*))$ ▷ Local Prediction

which defines the mean of \mathbf{X} as its first point, then sequentially defines the rest of the order based on which point has the greatest minimum distance to any point already in the set. That is, given an existing ordering on \mathbf{x}_i for $i \in \mathcal{I}$, the point

$$\underset{\mathbf{x}}{\text{argmax}} \min_{i \in \mathcal{I}} \|\mathbf{x}_i - \mathbf{x}\| \tag{A2}$$

is given the rank $|\mathcal{I}| + 1$. Algorithm 5 gives pseudo-code for the Vecchia approximation.

Algorithm 5 Vecchia Approximation to Gaussian Process Regression

Given: Prediction location \mathbf{x}^* ; Conditioning set size **nCond**

- 1: $\mathbf{X}_p \leftarrow \text{MaximinPermute}(\mathbf{X})$ ▷ Reorder the data
- 2: **for** $i \in \{1, \dots, n\}$ **do** ▷ Find ordered Nearest Neighbors, respecting order
- 3: $\mathcal{C}_i \leftarrow \text{OrderedNearestNeighbors}(\mathbf{X}_p, \text{nCond})$
- 4: **end for**
- 5: **fit** $\leftarrow \text{VecchiaGP}(\mathbf{X}_p, \mathcal{C}, \mathbf{y}(\mathbf{X}_p))$ ▷ Inference on approximate model
